Evaporation from Irrigation Canals in the Middle Reaches of the Heihe River in the Northwest of China : A Preliminary Study

Wang, Weizhen
Cold and Arid Regions Environmental and Engineering Institute, CAS

Liu, Suhua
Cold and Arid Regions Environmental and Engineering Institute, CAS

Kobayashi, Tetsuo
Cold and Arid Regions Environmental and Engineering Institute, CAS

Kitano, Masaharu
Laboratory of Agricultural Meteorology, Division of Bioproduction Environmental Sciences, Department of Agro-environmental Sciences, Faculty of Agriculture, Kyushu University

Evaporation from Irrigation Canals in the Middle Reaches of the Heihe River in the Northwest of China – A Preliminary Study–

Weizhen WANG[1], Suhua LIU[1], Tetsuo KOBAYASHI[1] and Masaharu KITANO*

Laboratory of Agricultural Meteorology, Division of Bioproduction Environmental Sciences,
Department of Agro–environmental Sciences, Faculty of Agriculture,
Kyushu University, Fukuoka 812–8581, Japan
(*Received April 25, 2013 and accepted May 9, 2013*)

In the northwest of China, the leakage and evaporation from irrigation canals is an important issue from the stand point of efficient use of water resources, because long canals have been constructed for farmland irrigation. In order to estimate the evaporation from irrigation canals a preliminary study was conducted in the middle reaches of the Heihe River during the summer months based on the heat balance method. The rate of evaporation from irrigation canals depends on the temperature difference between canal water and air, the air humidity, and the wind speed. The present observations showed that the seasonal variations of the temperature difference and the wind speed were not large in the observation period, and the seasonal variation of air humidity had a large influence on the evaporation rate. Since the Heihe River rises from the Qilian Mountains and the river water is melt–water, the water temperature is rather low compared to the air temperature. As a result, daily evaporation depth was often almost zero or negative. The results of this study were obtained by applying the relationship between the heat transfer coefficients and the surface wind speed empirically derived by Mihara *et al.* (1959b), so the results are only approximate. Hence, these results should be verified against observational evidence before a final conclusion can be drawn.

Key words: evaporation, heat balance method, Heihe River, irrigation canal

INTRODUCTION

If irrigation canals are unpaved ditches, we can conceive that a considerable amount of irrigation water is lost due to the leakage into the ground through the bottom and side wall of canals during its transport from a sluice gate to fields (Huang *et al.*, 2010).

In China, irrigation canals are classified into five groups; that is, *gan qu* (main canal), *zhi qu* (branch canal), *dou qu* (lateral canal), *nong qu* (field canal), and *mao qu* (field ditch). In the present study area, the middle reaches of the Heihe River (Fig. 1), the main and branch canals extending for 4,700 km have been paved. The total length of the lateral and field canals is 14,000 km, and the lateral canals have almost been paved and 30% of the field canals have been paved. In other words, water is leaking mainly from field canals and field ditches; that is, the leakage occurs mostly in or near irrigated fields, not in transport from an intake upriver to the irrigated fields.

In arid regions, however, the evaporation from the water surface of irrigation canals should be responsible for the loss. Since it is difficult to measure the evaporation from a limited land surface with a surface condition different from the surrounding area, and also to apply the evaporation pan or the lysimeter to running water surfaces, few researches and investigations into this subject have been carried out.

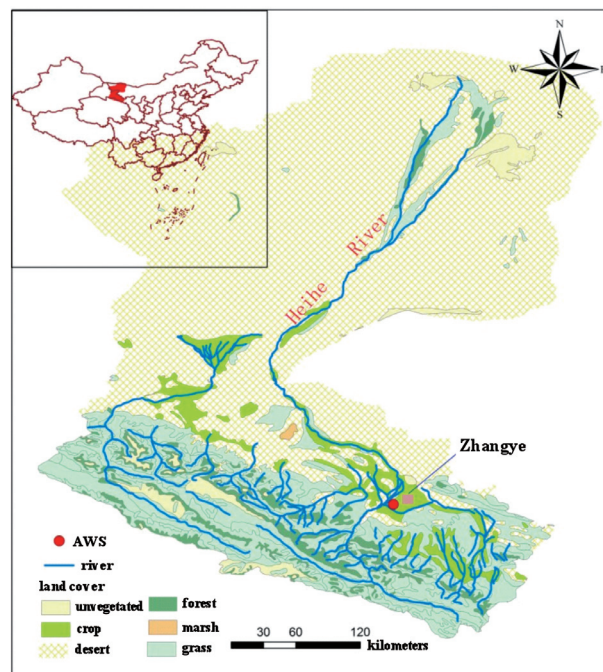In the late 1940s and early 1950s, the north or highland regions of Japan suffered the damage caused by cold

Fig. 1. Map of the Heihe River basin in the northwest of China.

weather to the paddy rice. The cold irrigation water arrests the paddy rice to grow and decreases its yield. Therefore, many water–warming ponds and canals were constructed. Mihara *et al.* (1959a) conducted a study of the heat balance of the water warming ponds (1959a). As a sequel to the study they also studied the heat balance of the water warming canals (1959b) in order to determine the rate of heat transfer between the running water surface and the surface air layer, and to make clear the characteristics of heat balance of the canal and

[1] Cold and Arid Regions Environmental and Engineering Institute, CAS, China
 * Corresponding author (E–mail: kitano@bpes.kyushu–u.ac.jp)

the change in temperature of the flowing water in the canal. As a result, they found that the water in the canals was warmed more by sensible and latent heat fluxes than by net radiation; that is, they estimated that not only sensible heat flux but also latent heat flux were negative or downward over the water surface in the canal. They also derived empirically the sensible and latent heat transfer coefficients as functions of the wind velocity.

This paper describes the method for estimating the latent heat flux over the water surface of a canal based on the heat balance analysis of the water flowing in the canal; in addition, the results of a preliminary study of the evaporation from irrigation canals in the middle reaches of the Heihe River in the northwest of China (Fig. 1) by applying the sensible and latent heat transfer coefficients as functions of the surface wind velocity obtained by Mihara *et al.* (1959b), so the results are only approximate.

HEAT BALANCE METHOD

Firstly, the heat balance method for estimating the evaporation from the water surface of an irrigation canal is outlined as an introduction to our application.

Figure 2 shows the schematic of a part of irrigation water flowing in a canal with rectangular cross section, being B (m) in width, L (m) in length, and D_w (m) in water depth. This is the water body element of which the heat balance is examined. It is assumed that the flow speed V (m s^{-1}) or discharge (m^3 s^{-1}) is invariable with the distance along the flow direction (x–direction), or water leakage and evaporation are negligible, and the temperature T_w (K) of the water flowing into the volume element at x=0 is $T_{w,in}$, and that of the water flowing out of the element at x=L is $T_{w,out}$. The net radiation, sensible heat flux, latent heat flux, and ground heat flux, are expressed by R_N, H, λE, and G, given in W m^{-2}, respectively. Here, the direction of an arrow in Fig. 2 points the positive direction of each term.

The energy balance of the water body element during a period of time, Δt (s), is described as follows, if the heat flux through the side wall is negligible:

$$c\rho V(T_{w,in} - T_{w,out})BD_w \; \Delta t + R_N LB\Delta t$$
$$= c\rho \frac{\partial T_W}{\partial t} LBD_w \Delta t + (H + \lambda E + G)LB\Delta t \qquad (1)$$
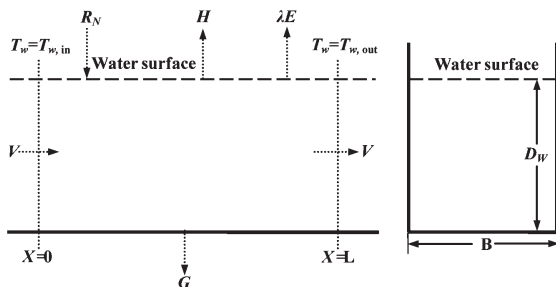

Fig. 2. Heat balance of water flowing in an irrigation canal. A side view (left) and a cross–sectional view (right). See text for explanation.

where $c\rho$: heat capacity of liquid water (J m^{-3} K^{-1}). This equation can be rewritten as:

$$c\rho Q(T_{w,in} - T_{w,out}) + [R_N]$$
$$= c\rho \frac{\partial T_W}{\partial t} LBD_w \Delta t + [H] + [\lambda E] + [G] \qquad (2)$$

where $Q \equiv VBD_w \Delta t$ (m^3) is the flow, and the flux terms $[X] \equiv XLB\Delta t$ (J). Since the water temperature is empirically known to change linearly with time, if the mean water temperature of the volume element is expressed as $T_{w,m} = \frac{1}{2}(T_{w,in} - T_{w,out})$, the first term on the right side of Eq.(2) is given as follows.

$$c\rho \frac{\partial T_W}{\partial t} LBD_w \Delta t = c\rho LBD_w \{T_{w,m}(t + \Delta t) - T_{w,m}(t)\} \quad (3)$$

The net radiation $[R_N]$ is measured or calculated as follows.

$$[R_N] = [R_{S\downarrow}] - [R_{S\uparrow}] + [R_{L\downarrow}] - [R_{L\uparrow}]$$
$$= [R_{S\downarrow}](1 - \alpha) + \varepsilon\{[R_{L\downarrow}] - [\sigma T_{w,m}^4]\} \qquad (4)$$

where $R_{S\downarrow}$: short wave downward radiation, $R_{L\downarrow}$: long wave downward radiation, $R_{S\uparrow}$: short wave upward radiation, $R_{L\uparrow}$: long wave upward radiation, α: albedo of the water surface, ε: emissivity of the water surface, σ: Stefan–Boltzmann constant.

The ground heat flux $[G]$ is measured directly with heat flux plates or calculated based on the ground temperature measurements. Let us assume that the soil temperature below the bottom of a canal is expressed as (Kobayashi, 2012):

$$\theta(z,t) = \theta_m(z) + A(0)\exp(-z/D)\sin(\omega t + \phi_0 - z/D) \qquad (5)$$

where z: depth below the bottom (positive downward) (m), D: damping depth ($= 2\alpha/\omega)^{\frac{1}{2}}$ (m), α: thermal diffusivity (m^2 s^{-1}), ω: angular frequency. Then we get

$$G = -k\left(\frac{\partial\theta}{\partial z}\right)_{z=0} = -k\frac{\partial\theta_m(z)}{\partial z}$$
$$+ A(0)(k\rho_S C_S \omega)^{\frac{1}{2}}\sin(\omega t + \phi_0 + \frac{\pi}{4}) \qquad (6)$$

where k: heat conductivity (W m^{-1} K^{-1}), $\rho_S C_S$: heat capacity of the soil (J m^{-3} K^{-1}). If Δt is one day, we can approximately get $[G] = [-k\frac{\partial\theta_m(z)}{\partial z}]$. The heat flux through the side wall is approximately estimated to be $\delta \equiv 2Dw/B$ times as large as that through the bottom.

The sensible and latent heat fluxes, $[H]$ and $[\lambda E]$ are obtained from the residual term of the heat balance equation:

$$[Res] \equiv [H] + [\lambda E] = c\rho Q(T_{w,in} - T_{w,out})$$
$$+ [R_N] - c\rho LBD_w \frac{\partial T_w}{\partial t}\Delta t - [G] \qquad (7)$$

Here the residual term $[Res] \equiv [H]+[\lambda E]$ is divided into $[H]$ and $[\lambda E]$ in the ratio of $\bar{\beta}$ to one, where $\bar{\beta}$ is the time averaged Bowen ratio for the period Δt; that is,

$$\bar{\beta} \equiv \frac{[H]}{[\lambda E]} \approx \frac{1}{n} \sum_{i=1}^{i=n} \gamma \left(\frac{T_a-T_w}{e_a-e_s(T_w)} \right)_i \qquad (8)$$

Here, n: number of measurements during Δt, $\gamma = \frac{PC_p}{0.622 \lambda}$: psychrometric constant (hPa K^{-1}), $e_s(T)$: saturated vapor pressure at temperature T (hPa), and other symbols have their usual meaning. Then we obtain

$$[H] = \frac{\bar{\beta}}{1+\bar{\beta}} [Res] \qquad (9)$$

$$[\lambda E] = \frac{1}{1+\bar{\beta}} [Res] \qquad (10)$$

MATERIALS AND METHODS

Study area

The study area is located in the Zhangye oasis (1,400–1,600 m a.s.l.), Gansu, China, which is the core part of the middle reaches of the Heihe River (Fig. 1). The annual mean temperature is 7.0 C and the annual mean precipitation is 124.9 mm. The potential evaporation is much larger than the precipitation, which is more than 2,000 mm. Main crops cultivated in this area are corn, wheat, and others, such as vegetables and fruits. Almost all the farmland in this area is irrigated with the water conducted from the Heihe River.

Preliminary observations

Meteorological measurements used in this study were made at AWS No.5 and No.11 (1500 m a.s.l.) of the

Fig. 3. The cross section of the canal and the measurements points of water flow speed and temperature.

HiWATER project (Li *et al.*, 2012). Table 1 shows the general description of a part of the instruments installed at the AWSs.

When irrigations were practiced, the observation of the water temperature and flow speed was conducted at a *dou qu* (lateral canal) site, which was situated about 500 m from the AWSs. In 2012, the preliminary observation was carried out three times during the periods of 22–24 June, 21–24 July, and 13–15 August. Fig. 3 shows the cross section of the canal and the measurement points of water flow speed and temperature.

Fundamental equations

The sensible heat flux from the water surface is expressed as:

$$H = \frac{1}{r_{ah}} \rho_a C_p (T_w - T_a) = K_h (T_w - T_a) \qquad \text{(W m}^{-2}\text{)} \quad (11)$$

where $\rho_a C_p$: specific heat capacity of the air (J m^{-3} K^{-1}), r_{ah} is the aerodynamic resistance for sensible heat transfer through the surface air layer, and K_h is the sensible heat transfer coefficient (W m^{-2} K^{-1}).

Latent heat flux from the water surface is expressed as:

$$\lambda E = \frac{1}{r_{av}} \lambda (\rho_v(T_w) - \rho_v(T_a)) = \frac{1}{r_{av}} \frac{\rho_a C_p}{\gamma} (e_s(T_w) - e_a)$$
$$= K_v (e_s(T_w) - e_a) \text{ (W m}^{-2}\text{)} \qquad (12)$$

where $\rho_v(T_w)$, $\rho_v(T_a)$: water vapor densities at the water surface and in the surface air layer, respectively, K_v: water vapor transfer coefficient (W m^{-2} hPa^{-1}). If we suppose the aerodynamic resistance for vapor transfer through the surface air layer, r_{av}, is equal to r_{ah}, we get the following relation from Eqs.(11) and (12):

$$K_v = \frac{1}{r} K_h \qquad (13)$$

Mihara *et al*. (1959b) empirically derived the relationship between the heat transfer coefficients, K_h and K_v, and the wind speed at 2 m height, U_2 (m s^{-1}). They set Δt to be one hour (3,600 s) and the number of measurements during Δt, n, to be one; that is, they obtained K_h and K_v every hour, when they used the 2–min mean of the wind speed.

Since $K_h = \frac{1}{r_{av}} \rho_a C_p$, this coefficient depends on the air pressure. Further, because γ is proportional to the air pressure (=0.000646P hPa K^{-1}), the relation of K_v to the air pressure is more complicated. So, strictly speaking,
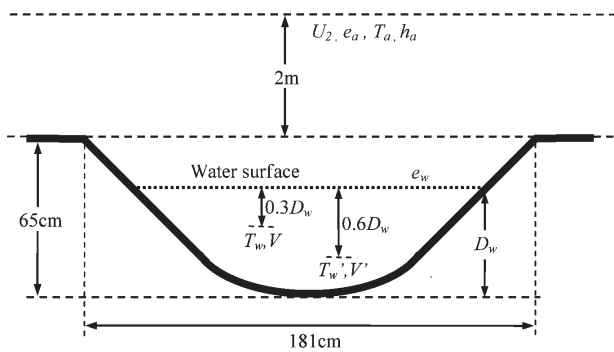
Table 1. Description of a part of the instruments installed at the AWS

Variables	Instruments	Observation Frequency (miu.)	Height & Depth (m)
Air Temperature & Humidity	HMP45AC (VAISALA)	10	5
Wind Speed	010C–1 (MET ONE)	10	10
Atmosphere Pressure	CS100 (VAISALA)	10	1.2
Water Temperature & Speed	Flowatch (NTECH)	–	–0.15

their empirically derived relationships are applicable only to the area where the air pressure is almost the same as their observation site (about 200 m a.s.l.) (Mihara *et al.*, 1959b).

The altitude of the present study area is about 1,500 m a.s.l., and hence the air pressure is, on average, about 85% of that at their observation site. However, as a first approximation, we assumed K_h to be applicable to our study area and K_v was obtained from the relationship between them as shown in Eq.(13); that is,

$$K_h = 4.0 + 3.1 U_2 \qquad (14)$$

$$K_v = \frac{1}{0.000646 P} (4.0 + 3.1 U_2) \qquad (15)$$

where P : air pressure (hPa).

This relationship was derived using the data obtained in the daytime when the vertical profile of air temperature was super–adiabatic, that is, the vertical air temperature gradient was larger than the dry–adiabatic lapse rate (0.0098 K m^{-1}). Hence, H and λE should be overestimated at night if Eq.(14) is used.

Thus, the rate of evaporation from the irrigation canal is given by

$$E_{ic} = \frac{1}{\lambda \rho_w} \frac{1}{0.000646 P} (4.0 + 3.1 U_2)(e_s(T_{w,ic}) - e_a) \\ (\text{m s}^{-1}) \qquad (16)$$

where $T_{w,ic}$: water temperature in the irrigation canal, λ: heat of water vaporization at the temperature $T_{w,ic}$ ($\approx 2.5 \times 10^6$ J kg^{-1}), ρ_w: density of liquid water (kg m^{-3}).

The amount of irrigation water lost in transport due to evaporation, L_{ev}, and the loss ratio due to evaporation of irrigation water, LR_{ev}, are defined as:

$$L_{ev} = \int_0^{t_t} E_{ic} dt \qquad (\text{m}) \qquad (17)$$

$$LR_{ev} = \frac{L_{ev}}{\mu D_w} \qquad (-) \qquad (18)$$

where t_t: time for water transport (=canal length/V)(s), μ: cross–section shape factor (–) μ=1/2, if triangle; μ=1, if rectangle).

RESULTS AND DISCUSSION

Table 2 shows the weather conditions and the daily mean flow speed in the canal during the periods of preliminary observation. Observations of meteorological elements are the averages of the two AWSs. Water flow speed and temperature were measured a few times a day at the two depths, 0.3 D_w and 0.6 D_w, where D_w is the water depth in the canal, which averaged about 40 cm (Fig. 3). However, because the diurnal changes in the temperature and flow speed and the differences between the measurements made at the two depths were small, the daily mean of the measurements made at 0.3 D_w was used in this study.

Using the meteorological observations taken at an interval of 10 minutes and the daily mean water temperature, we calculated E_{ic} from Eq.(16). Fig. 4 illustrates the diurnal changes of E_{ic} in three days of June. The values on the ordinate are given in units of 10^{-5} mm s^{-1}, which is equivalent to 0.86 mm d^{-1}. The diurnal changes on 22 and 24 June were similar to each other. The magnitude of the cumulative evaporation depth in the daytime (8:00–20:00) was about twice as large as that in the nighttime (20:00–8:00) on both days, while on 23 June the cumulative depths by day and at night were almost the same as shown in Fig.6.

Figure 5 shows the diurnal changes in air temperature and relative humidity on 22 and 23 June. During two periods between 21:00 and 24:00 of 22 June and 5:00 and 7:00 of 23 June, when the evaporation rate was rather large, relative humidity was low, although air temperature and wind speed remained nearly constant. In the daytime of 23 June, relative humidity was, as would be expected, higher than that of 22 June, and the evapora-

Table 2. Weather conditions and the daily mean flow speed in the canal during the periods of preliminary observation

| Date	Air temper.* at 2 m (°C)	Air humid.* at 2 m (%)	Wind speed* at 2 m (m s^{-1})	Solar radiation (MJ m^{-2} d^{-1})	Rainfall (mm d^{-1})	Flow speed* (m s^{-1})
22 June	23.5	36.6	1.81	23.1	–	2.8
23 June	20.1	51.8	1.81	16.2	–	2.8
24 June	21.1	41.4	1.14	30.1	–	2.6
21 July	20.8	69.9	0.95	25.8	2.5	2.5
22 July	20.4	60.5	1.37	15.3	–	2.5
23 July	19.8	58.6	1.62	18.7	–	2.5
24 July	18.8	70.4	1.01	16.9	–	2.5
13 August	19.8	77.3	1.08	14.4	1.5	2.6
14 August	20.9	68.3	0.89	26.2	0.1	2.6
15 August	22.4	49.4	1.29	23.9	–	2.5

* Daily mean.
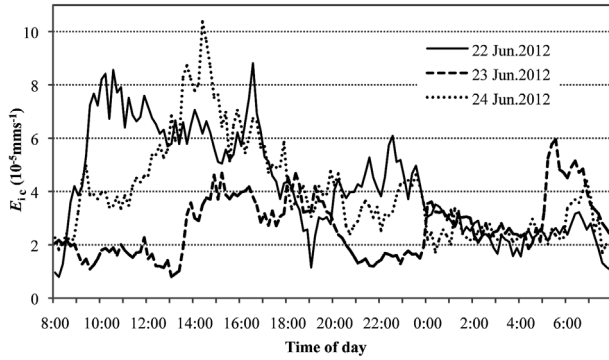
Fig. 4. Diurnal changes of E_{ic} in three days of June.
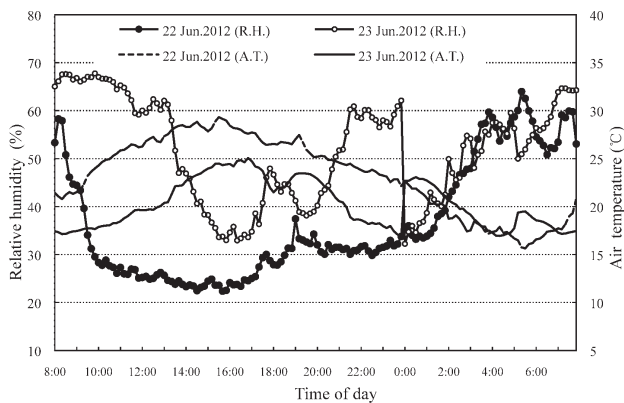
Fig. 5. Diurnal changes in air temperature and relative humidity on 22 and 23 June.

Fig. 6. Day–to–day changes of the daytime (white), nighttime (black), and daily cumulative evaporation depth (gray).

Fig. 7. Seasonal changes in the daily mean air temperature, relative humidity, and the water temperature in the canal.

tion rate during the day of 23 was much smaller than that of 22 June. These results suggest that the evaporation from the irrigation canal is very sensitive to the air humidity.

Figure 6 shows the day–to–day changes of the daytime (white), nighttime (black), and daily cumulative evaporation depth (gray). Contrary to expectation, the maximum of daily evaporation depth from irrigation canals occurred in June, and daily evaporation was often almost zero or negative in July and August.

Figure 7 shows the seasonal changes in the daily mean air temperature, relative humidity, and the water temperature in the canal. Although the water temperature showed a slight increase during the summer months, it does not seem to exert its influence on the evaporation rate. Neither daily mean air temperature nor wind speed showed large seasonal changes during this period of time, but relative humidity was lower in the middle of and late in June, and late in August, than the other times. As for the diurnal variation of the rate of evaporation from irrigation canals, also for the seasonal variation, air humidity seems to have been the most important factor that controlled the evaporation rate.

Although, at first glance, the condensation of water vapor on the water surface may be strange, whether evaporation occurs or condensation occurs depends on the numbers of water molecules emitted from and received by the water surface. Thus, it is not strange that conden-
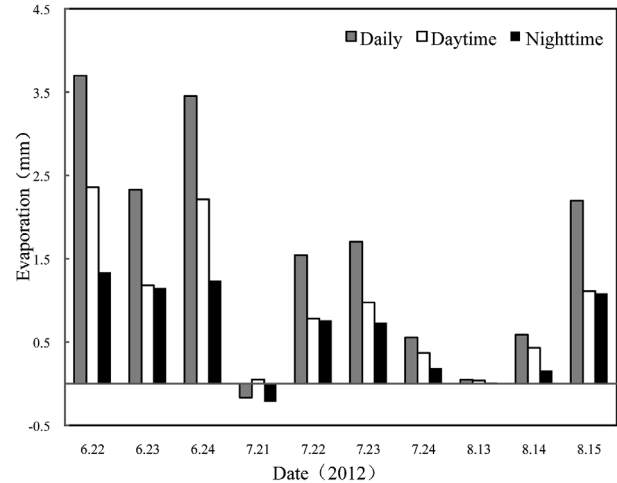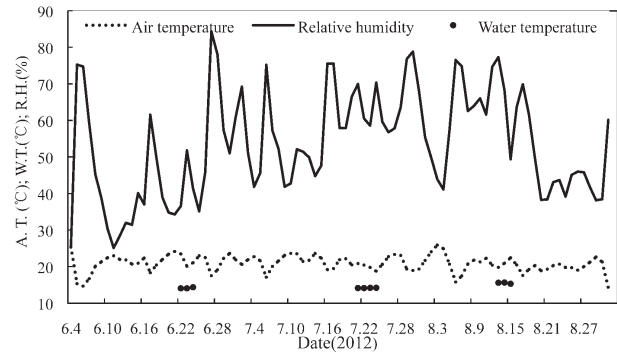
sation occurs when the water temperature is low enough relative to the air humidity.

Lastly, let us estimate L_{ev} and LR_{ev} defined by Eqs. (17) and (18). If D_w=40 cm, μ=1/2, t_t=one day, and E_{ic} obtained on 22 June 2012 is used, L_{ev}=3.7 mm and LR_{ev}=0.02. As mentioned above, the results obtained in this study are only approximate, but the loss of irrigation water due to evaporation seems to be an order of magnitude smaller than the water loss due to the leakage into the ground from the whole canal network, because Fipps (2000, as cited by Huang *et al.*, 2010) estimated that the Rio Grande region (region M) had an average conveyance efficiency of 70% or 30% of the amount of irrigation water was lost due to the leakage.

CONCLUDING REMARKS

The rate of evaporation from irrigation canals depends on $\Delta T = T_w - T_a$, air humidity, and U_2. In the period of the present preliminary observation, the variations of ΔT and U_2 with time were not so large, and hence air humidity had a large influence on the evaporation rate. Since the Heihe River rises from the Qilianshan Mountains and the river water is melt–water, T_w is rather low compared to the air temperature. As a result, daily

evaporation depth was often almost zero or negative. Although K_h is related to the air pressure, Eq.(14) obtained in lowland areas (about 200 m a.s.l.) in Japan was, as a first approximation, used to the present case in this highland area (about 1,500 m a.s.l.) in the north west of China. Since K_v depends on the air pressure in a complicated manner, the approximate relation as shown in Eq.(13) was used and the empirical relation given by Mihara *et al.* (1959b) was not applied to this case. However, these estimates are only approximate and should be verified against observational evidence before a final conclusion can be drawn. We are planning to do such an experiment in the next irrigation season. However, it seems reasonable to say that the loss of irrigation water due to evaporation should be an order of magnitude smaller than the water loss due to the leakage into the ground from the whole canal network.

ACKNOWLEDGRMENTS

REFERENCES

Huang, Y., G. Fipps, S. J. Maas and R. S. Fletcher   2010 Airbone remote sensing for detection of irrigation canal leakage. Irrig. and Drain., **59**: 524–534

Kobayashi, T. 2012 *Physics of Agricultural Environment*. Cold and Arid Regions Environmental and Engineering Institute, CAS.

Li, X., Liu, S., Ma, M., Xiao, Q., Liu, Q., Jin, R., Che, T., Wang, W., Qi, Y., Li, H., Zhu, G., Guo, J., Ran, Y., Wen, J., Wang, S.,   2012 HiWATER: An integrated remote sensing experiment on hydrological and ecological processes in the Heihe River Basin. Advances in Earth Science, 2012, **27**(5): 481–498 (in Chinese)

Mihara, Y., Z. Uchijima, S. Nakamura and K. Onuma   1959a   A study on heat balance and water temperature rising of the warming pond. *Bulletin Nation. Inst. Agric. Sci., Japan*, A–7: 1–44. (in Japanese with English summary)

Mihara, Y., Z. Uchijima and S. Nakamura   1959b   A study on heat balabce of the water warming channels. *Bulletin Nation. Inst. Agric. Sci., Japan*, A–7: 45–68 (in Japanese with English summary)